

# Electrochemical synthesis and characterization of zinc selenide thin films

T. MAHALINGAM

*Department of Physics, Alagappa University, Karaikudi – 630 003, India; Department of Electrical and Computer Engineering, College of Information Technology, Ajou University, Suwon 443-749, S. Korea*

A. KATHALINGAM\*

*Department of Physics, Periyar Maniammai College of Technology for Women, Vallam, Thanjavur – 613403, India*

S. VELUMANI

*Mexican Institute of Petroleum, Eje Central 152, C.P. 07730, México, D.F, Mexico*

SOONIL LEE

*Department of Molecular Science and Technology, Ajou University, Suwon 442-749, S. Korea*

M. H. SUN, K. Y. DEAK

*Department of Electrical and Computer Engineering, College of Information Technology, Ajou University, Suwon 443-749, S. Korea*

**Published online:** 12 April 2006

---

In this work, electrochemical deposition and characterization of zinc selenide (ZnSe) thin films is reported. ZnSe thin films were deposited onto tin oxide (SnO<sub>2</sub>) coated conducting glass substrates from an aqueous solution bath containing ZnSO<sub>4</sub> and SeO<sub>2</sub>. The effect of deposition parameters such as bath temperature, deposition time and electrolyte composition on the properties of the ZnSe films has been studied. Cyclic Voltammetric studies were carried out to optimize the deposition potential for the co-deposition of Zn and Se. Deposited ZnSe films have been characterized by X-ray diffraction (XRD), energy dispersive X-ray (EDX), scanning electron microscope (SEM) and optical techniques for their structural, compositional and optical properties and the results are discussed. © 2006 Springer Science + Business Media, Inc.

---

## 1. Introduction

Binary semiconductors are considered as important technological materials due to their potential applications in various optical and electronic devices. Zinc selenide (ZnSe), a direct and wide band gap (2.7 eV) [1] II–VI compound, has been widely studied because of its potential use in semi conducting and optoelectronic devices and as window material for thin film heterojunction solar cells. Due to its very wide transmission range and high optical quality, it is used to manufacture optical components, mirrors, lenses etc for IR lasers [2]. ZnSe films are usually prepared by vapor phase epitaxy [3], atomic layer epitaxy [4], metalorganic chemical vapor deposition [5], sputtering [6], chemical bath deposition [7], etc. Electrodeposition technique has been found to be a useful method to

prepare polycrystalline semiconducting films for the use in photovoltaic cells. Electrodeposition technique seems to be an inexpensive, low temperature method that could produce good quality films for device applications. The attractive features of this method are the convenience for producing large area devices and possibility to control the film thickness, morphology and stoichiometry of the films by readily adjusting the electrical parameters, as well as the composition of the electrolyte solution. In general, electrodeposition of an alloy or a compound is a very complex, involving thermodynamics and kinetics problems. Though the ZnSe has been explored large in bulk and thin film state, there is less quantum of work in the case of electrodeposition of ZnSe thin films. In this paper, we report the electrodeposition of ZnSe thin films from

\*Author to whom all correspondence should be addressed.

an aqueous solution bath containing  $\text{ZnSO}_4$  and  $\text{SeO}_2$ . The potentiostatic method was chosen to permit stoichiometric control, but the effect of galvanostatic deposition was also studied. The influence of growth conditions such as deposition potential, temperature on crystallinity and composition of the film was studied. SEM, XRD, EDAX and optical transmission techniques were employed for characterizing the deposited films.

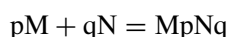
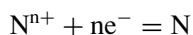
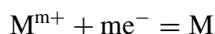
## 2. Experimental details

Deposition of the films was carried out electrochemically by co-deposition of zinc and selenide using fluorine doped tin oxide ( $\text{SnO}_2$ ) coated conducting glass plates (15 ohms/square) as substrates. Tin oxide substrates of approximately  $1 \text{ cm}^2$  area were cleaned with detergent, dried and degreased with acetone and distilled water. The electrolyte bath contained an aqueous solution of AnalaR grade 50 to 300 mM  $\text{ZnSO}_4$  and 0.2 to 2 mM  $\text{SeO}_2$ . Deposition was carried out cathodically using a potentiostat (EG & G Princeton Applied Research, Model 362) with standard three-electrode arrangement such as working electrode (substrate), counter electrode (graphite rod) and a saturated calomel electrode (SCE) as reference electrode. Depositions were carried out at different potentials ranging from  $-0.4 \text{ V}$  to  $-1.2 \text{ V}$  versus SCE at different bath temperatures. The pH of the electrolyte was kept between 2 and 3. Dilute  $\text{H}_2\text{SO}_4$  was used to adjust the pH value of the solution bath. To characterize the electrochemical behavior of the Zn/Se system in acid solutions, a detailed Cyclic Voltammetric (CV) study of the precursors and their mixtures was firstly accomplished. CV studies are used to select the potential for one step electrodeposition of ZnSe thin films at constant potential. Galvanostatic deposition was also studied by varying current and bath concentrations. The thickness of the film was measured using weight gain and ellipsometric methods. The structure and composition of the films were analyzed using X-ray diffraction (XRD) by Bruker Discover D8 diffractometer using  $\text{Cu } k_\alpha$  radiation with  $\lambda = 0.15418 \text{ nm}$  and Philips scanning electron microscope (SEM) attached with energy dispersive X-ray unit (EDAX).

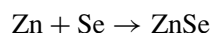
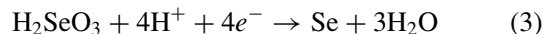
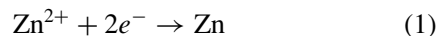
## 3. Results and discussion

### 3.1. Deposition kinetics

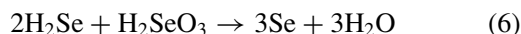
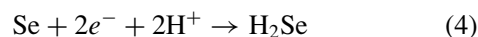
The deposition of ZnSe by electrodeposition is more difficult than the other cadmium chalcogenide semiconductors. The generalized form of cathodic deposition of a compound semiconductor from two elements Mp and Nq is described as follows.



More specifically, for the electrodeposition of ZnSe



Number of side reactions as mentioned below can also take place and influence the nature of the grown films depending on the growth conditions.



Uniform and good quality films were found to grow in the following optimized deposition conditions: Deposition potential:  $-0.9 \text{ V}$  vs SCE, Current density:  $1 \text{ mA cm}^{-2}$ ,  $\text{ZnSO}_4$  concentration: 0.3 M,  $\text{SeO}_2$  concentration: 1 mM and bath temperature  $70^\circ\text{C}$ . The color of the film was found to be gray but initially when deposition was undergoing it appeared as brownish red. When the current increases to  $10 \text{ mA cm}^{-2}$  more bubbles were evolved and this may be attributed to the hydrogen evolution via the reaction (5). Uniform and adherent films were obtained when the solution pH is in the range between 2 and 3. When the pH is higher than 4, a non-uniform coating with a very thin layer was deposited. This may be attributed to the poor conductivity of the electrolyte at higher pH values. When the solution pH is less than 1, the deposited film is not adhered with the substrate. Hence, we have prepared our samples at a pH of 2.5 throughout the investigation of the present work. Fig. 1 shows the variation of film thickness with deposition time for ZnSe thin films

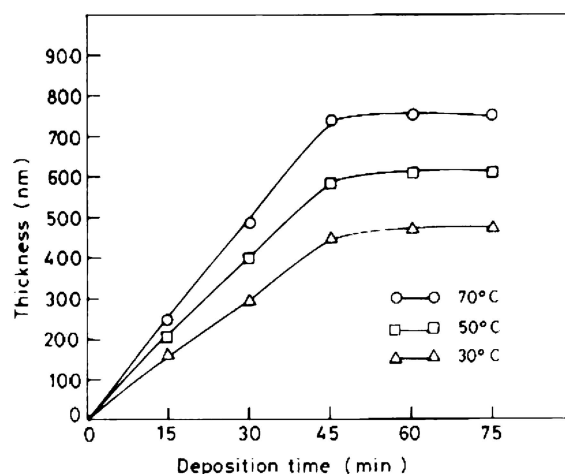


Figure 1 Variation of film thickness with deposition time at various bath temperatures (Bath composition: 300 mM  $\text{ZnSO}_4$  and 1 mM  $\text{SeO}_2$ , Deposition potential  $-0.9 \text{ V}$  vs SCE).

prepared at three different bath temperatures. As the deposition time increases, the thickness is found to increase and reaches saturation around 450 nm at a deposition time of about 45 min for film deposited at bath temperature 30°C. Similar trend is observed for films deposited at bath temperatures 50°C and 70°C. The growth rate of the films deposited at 30°C, 50°C and 70°C are estimated to be 10, 13.3 and 16.3 nm, respectively. This value is found to be comparatively higher than the growth rate of 6 nm/min for ZnSe thin films prepared by chemical bath deposition [7]. The growth rate is high at initial stage, later it slowed down with time and attains saturation after 45 min of deposition. No film growth was observed after 60 min of deposition.

### 3.2. Voltammetric study

Electrochemical behavior of the Zn/Se system on SnO<sub>2</sub>/glass was studied by constructing voltammetric curves. In the case of ZnSe film growth, the electrolyte bath was an acidic aqueous solution (pH = 2.5) containing 300 mM ZnSO<sub>4</sub> and 1 mM SeO<sub>2</sub>, held at 70°C. The cyclic photovoltammetry technique consisted in examining the current response of the electrodeposit/electrolyte interface under conditions of voltammetric scanning and modulated light excitation. The electrode/electrolyte interface was illuminated with white light, which was manually chopped during voltammetric scanning. Thus, the photo response of the forming semiconductor serves as an in situ diagnostic probe of the deposition mechanism and product formation. This voltammetric study gives the information about the possible range of deposition potentials for the bath of different composition of Zn and Se. When applied potential is scanned towards negative values in acid solutions containing only Zn<sup>2+</sup>, the current contribution only is observed corresponding to that of hydrogen evolution reaction. When scanning towards negative potentials for SeO<sub>2</sub> solution, a reduction wave for selenous acid to Se centered at -0.4 V (Fig. 2a) and a reddish film deposition was observed according to the reaction (3). When both the precursors are present in the electrolyte bath, the reduction wave centered at -0.4 V is suppressed (Fig. 2b). Increase of cathodic current is observed from -0.7 V to -1.0 V when electrode is illuminated with white light. This appearance of a cathodic photocurrent soon after further decrease of the potential is ascribed to the formation of ZnSe [8]. According to Kroger's model the reduction of Zn<sup>2+</sup> above its redox potential (-1.02 V) is due to the gain of free energy by the formation of compound. Based on the above observations, we selected a potential range of -0.4 V-1.2 V for the deposition of ZnSe films.

### 3.3. Effect of bath temperature

Bath temperature usually affects the rate of electrodeposition and the film properties. The temperature is ex-

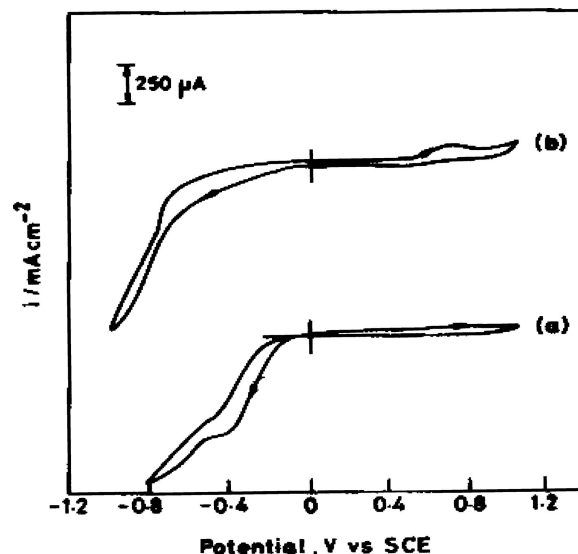


Figure 2 Cyclic voltammograms on SnO<sub>2</sub> coated glass: (a) 1 mM SeO<sub>2</sub>, pH 2.5, (b). 300 mM ZnSO<sub>4</sub> and 1 mM SeO<sub>2</sub>, pH: 2.5.

pected to influence the deposition rate by (i) increasing the diffusion coefficient, (ii) decreasing the viscosity and (iii) increasing the precursor solubility. ZnSe films deposited at room temperature were found to be poor in crystalline quality. High bath temperatures are usually necessary for achieving crystalline films in electrodeposition. However, the constant diffraction peaks of XRD patterns of the films deposited at various temperatures (50°C to 70°C) in the present study attribute that there was no major effect of bath temperature in the crystalline size of the films. Though the compositional study showed excess of selenium deposited at higher bath temperature, the XRD patterns did not show any presence of selenium. So, it is concluded that only amorphous selenium was incorporated into the film deposited at higher bath temperature.

### 3.4. Effect of deposition potential

Films were deposited at various deposition potentials starting from -0.4 V to -1.2 V vs SCE. During deposition, an excess of Se was encountered in the films. The best stoichiometry of the film was obtained at a deposition potential close to -0.9 V vs SCE. Fig. 3 shows XRD patterns obtained for the films deposited at potentials of -0.7 V, -0.8 V, -0.9 V, and -0.1 V versus SCE at bath temperature 70°C. These XRD patterns are compared with JCPDS data (No: 5-522) and it was confirmed that cubic polycrystalline ZnSe films were deposited. The diffraction peaks at 27.3°, 45.3°, 53.7° and 65.8° are attributed to the (111), (220), (311) and (400) planes respectively of cubic ZnSe [9, 10]. All the peak intensities are found to increase when the deposition potentials decreasing down to -0.9 V. When the deposition potential is further decreased to -1.0 V versus SCE, ZnSe diffraction peaks are disappeared. It indicates that ZnSe thin films

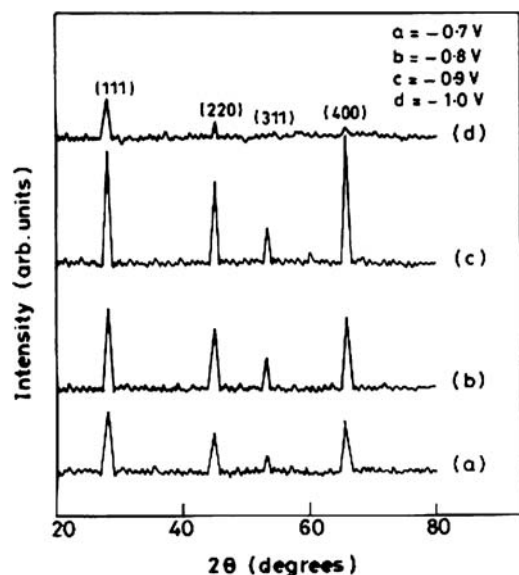


Figure 3 XRD Patterns of the films deposited at different potentials (Bath composition: 300 mM ZnSO<sub>4</sub>, 1 mM SeO<sub>2</sub>, pH = 2.5, Bath temperature: 70°C and plating time: 1 h).

with polycrystalline morphology are formed in the potential range between  $-0.7$  V and  $-0.9$  V versus SCE. The voltammograms presented above also demonstrate that ZnSe can be electrodeposited at a potential ranging from  $-0.5$  V to  $-1$  V versus SCE. The diffraction peaks are not found to be indicating very small crystalline sizes in the films. The crystallinity of the electrodeposits can be improved by annealing them at high temperatures. It is found that annealing of electrodeposited ZnSe films at  $300^{\circ}\text{C}$  for 45 min in air increased the intensity of the diffraction peaks and enhanced the crystallinity substantially.

The crystallite size ( $D$ ) is calculated using the Debye-Scherrer formula [11] from the Full Width at Half Maximum (FWHM)  $\beta$ ,

$$D = 0.94\lambda/\beta \cos \theta$$

where  $\lambda$  is the wavelength of the X-ray used,  $\beta$  is the FWHM and  $\theta$  is the diffraction angle. The crystallite size ( $D$ ) is estimated to be 9.5 nm for (111) plane of cubic ZnSe thin film deposited at a potential  $-0.9$  V versus SCE (Fig. 3) The dislocation density ( $\delta$ ) is calculated from the formula [12]

$$\delta = 1/D^2$$

and found to be  $1.1 \times 10^{16}$  lines/m<sup>2</sup>. This is in fair agreement with the value reported for electrodeposited cuprous oxide thin films [13].

The potential dependent composition of various electrodeposits is shown in Fig. 4. There was a major change of Zn/Se ratio for films deposited between  $-0.7$  V and  $-1$  V versus SCE. It is found that stoichiometric ZnSe film was

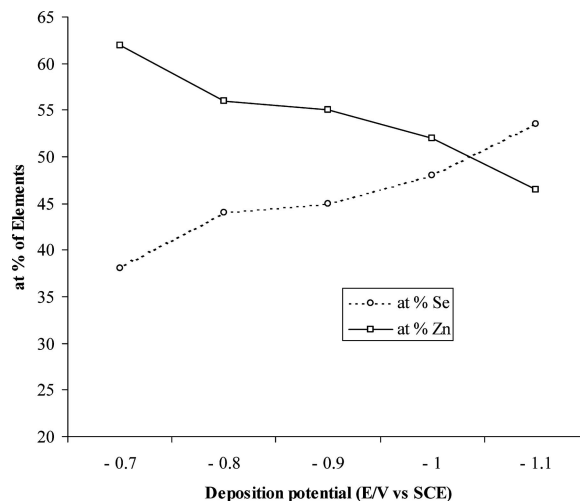


Figure 4 Variation of elemental composition (at%) of ZnSe thin films with deposition potential. (Bath composition: 300 mM ZnSO<sub>4</sub>, 1 mM SeO<sub>2</sub>, pH: 2.5, Bath temperature: 70°C and plating time: 1 h).

deposited for deposition potential around  $-0.9$  V versus SCE.

### 3.5. Effect of bath composition

In case of electrodeposition of ZnSe, the use of low concentration of selenous acid and high concentration of zinc salt is the usual approach. This is due to the fact that zinc is a less noble constituent of the compound. In this way, the rate of reaction (3), which is one of the paths for the incorporation of an excess of elemental selenium in the film, can be lowered. The film thickness linearly increases with both ZnSO<sub>4</sub> and SeO<sub>2</sub> concentrations. However, the increase is restricted to a very low concentration range and it gets saturated for higher concentration of both precursors. We observed less adherent, uncontrolled and non-reproducible growth rate for the concentration of ZnSO<sub>4</sub> above 300 mM. Films deposited at higher concentration of Zn<sup>2+</sup>, with the deposition parameters remaining unchanged, gave lower XRD peaks and an increasing current density was noticed.

Regarding the concentration of selenous acid, it should be in the lower level. However, too low concentration of the selenous acid gives low deposition rate and poor quality films. The compositional analysis of the film deposited with different SeO<sub>2</sub> concentration is shown in Table I. The low concentration of selenous acid only has yielded good

TABLE I

SeO <sub>2</sub> concentration (mM)	Zn/Se ratio (at%)
3	11/89
2.5	16/84
2	31/69
1.5	41/59
1	45/55

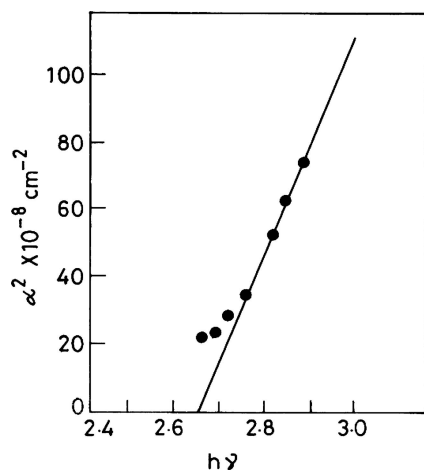


Figure 5 Variation of  $\alpha^2$  versus  $h\nu$  for a typical ZnSe film.

stoichiometric ratio in the ZnSe films. Hence, we selected the 300 mM of  $\text{ZnSO}_4$  and 1 mM of  $\text{SeO}_2$  as an optimum electrolyte concentration for further deposition and characterization of ZnSe films.

The inclusion of elemental selenium is unavoidable in the deposits [14] and the adsorption of  $\text{Zn}^{2+}$  is playing a vital role for obtaining stoichiometric films. If the adsorption sites were occupied by other species (ie  $\text{H}_2\text{SeO}_3$  or any other), the rate of  $\text{Zn}^{2+}$  reduction was reduced compared to  $\text{SeO}_2$  reduction. Thus Se cluster could be formed. If once the Se clusters have reached a certain size, it reacts slowly to give ZnSe.

### 3.6. Effect of galvanostatic deposition

In galvanostatic deposition, the inclusion of elemental selenium is large when compared with potentiostatic deposition. The optimum current density to obtain stoichiometric ZnSe films was found to be  $2 \text{ mA cm}^{-2}$ . At other current densities, poor crystalline quality films were obtained. However, annealing is found to improve the crystallinity of the films. At low current density ( $\leq 2 \text{ mA cm}^{-2}$ ), light brown coloured transparent deposition was observed. At high current density ( $\geq 5 \text{ mA cm}^{-2}$ ) thick and less adherent depositions were formed. A different morphology is also observed for galvanostatically deposited ZnSe films (Fig. 8c).

### 3.7. Optical studies

Optical transmittance and reflectance spectra were obtained for the films deposited at optimized conditions. The transmittance spectrum (result not shown) reveals a high transmission of 90% in the infrared region ( $\geq 700 \text{ nm}$ ) and a low transmission of 40% at 400 nm. Fig. 5 shows the  $\alpha^2$  vs  $h\nu$  plot of ZnSe film. The linear dependence showed by  $\alpha^2$  with  $h\nu$  indicates that this transition is direct. The band gap  $E_g$  value is calculated from the linear fit of the  $\alpha^2$  vs  $h\nu$  plot giving the value of 2.66 eV and it is found to be in good agreement with earlier reports [14]. It is known that the optical band gap of polycrys-

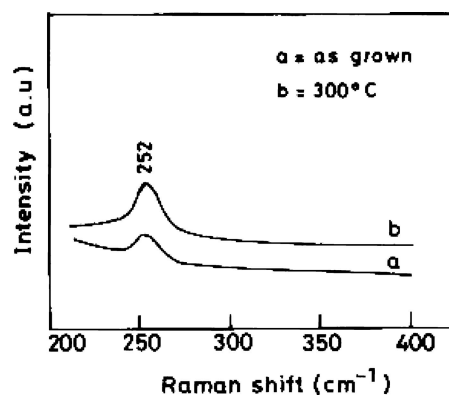


Figure 6 Raman spectra of as-grown and annealed ( $300^\circ\text{C}$  in air for 45 min) ZnSe films.

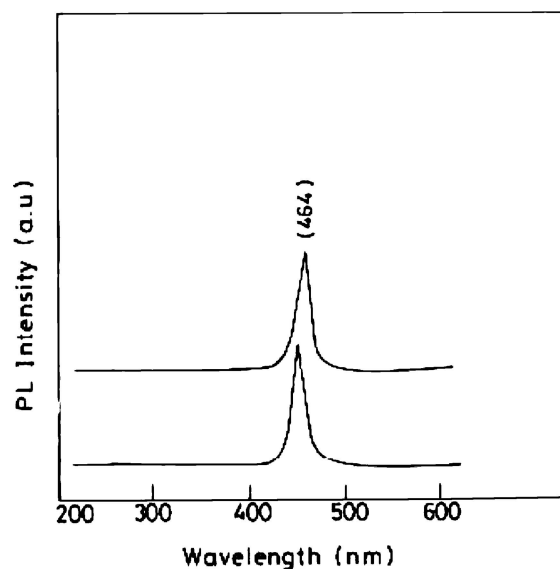


Figure 7 Room temperature photoluminescence spectra of ZnSe films for two different thicknesses.

talline ZnSe semiconducting thin film can be higher than that of bulk ZnSe ( $2.58 \text{ eV}$ ) due to quantum size effects. As the film grows thicker, there is ZnSe particulate adsorption at the film surface-giving rise to scattering losses, which is increasing with decrease of wavelength. Fig. 6 illustrates Raman spectra of the as-grown and annealed ZnSe films. The peak observed at  $252 \text{ cm}^{-1}$  for both as-grown and annealed film is due to the LO phonon of ZnSe [15, 16]. Although the amorphous Se exhibits an optical absorption at  $252 \text{ cm}^{-1}$ , the crystalline Se obtained after annealing has to exhibit  $240 \text{ cm}^{-1}$ . Hence, the observed peak at  $252 \text{ cm}^{-1}$  is assigned to the ZnSe. It confirms the formation of polycrystalline ZnSe films. The high peak obtained for annealed film shows increase of crystallite size due to annealing. Fig. 7 shows photoluminescence spectrum of as deposited ZnSe thin films. The peak located a  $464 \text{ nm}$  ( $2.68 \text{ eV}$ ) can be associated with the excitonic emission line [17, 18], and it is a fingerprint of good quality ZnSe film. The spectral position varies slightly with change of the film thickness.



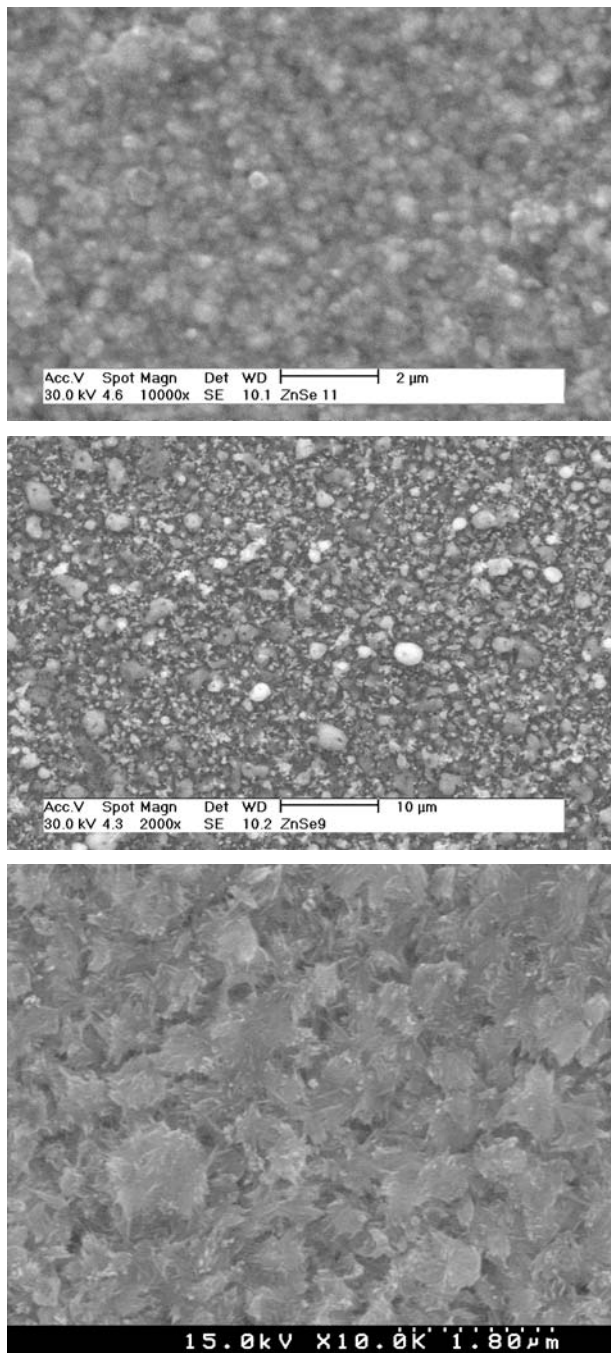


Figure 8 SEM micrograph of typical ZnSe films: (a) As-grown, (b) Annealed (350°C for 45 min), and (c) Galvanostatically grown.

### 3.8. Surface morphological studies

Fig. 8 shows the scanning electron micrographs obtained for the films deposited at various conditions. In optimised condition, the surface of the film is smooth showing grains well covering the substrate. The cross sectional view of the ZnSe film did not show presence of any voids or pinholes. Isolated islands are found, some larger spots are also observed but they are actually the aggregation of the smaller islands. The as-grown films (Fig. 8a) do not present well defined grain edges due to the excess selenium. However, when the films are subjected to

annealing (Fig. 8b) well-defined grains are fixed. Galvanostatically grown films (Fig. 8c) exhibits a dendrite growth pattern different from the potentiostatically grown films. Differences in terms of chemical composition are also observed in the morphology of the electrodeposited films.

## 4. Conclusion

Our studies show that ZnSe thin films could be grown using electrodeposition by appropriate selection of the growth parameters. The as-grown films presented excellent adherence and relatively good morphological and crystalline properties as inferred from SEM and XRD analysis. The bath temperature did not show any significant change in the XRD patterns of the films. It has been found that the ratio of  $[\text{ZnSO}_4]: [\text{SeO}_2]$  in the bath should be high in order to get a Zn/Se ratio close to 1 in the films. The films present either a gray or reddish brown colour depending upon the excess content of Zn or Se, respectively. Energy band gap of the film was estimated to be 2.66 eV and it is quite close to the reported value of 2.7 eV. Among galvanostatic and potentiostatic methods, the potentiostatic method was found most suited for the electrodeposition of ZnSe thin films.

## References

1. S. T. LAKSHMIKUMAR and A. C. RASTOGI, *Thin Solid Films*, **256** (1995) 150.
2. E. KRAUSE, H. HARTMANN, J. MENNINGER, A. HOFFMANN, CH. FRICKE, R. HEITZ, B. LUMMER, V. KUTZER and I. BROSER, *J. Cryst. Growth*, **138** (1994) 75.
3. A. RUMBERG, CH. SOMMERHALTER, M. TOPLAK, A. JAGER-WALDAU and M.CH. LUXTEINER, *Thin Solid Films*, **361/362** (2000) 172.
4. C. WANG, X. F. QIAN, W. X. ZHANG, X. M. ZHANG, Y. XIE, and Y. T. QIAN, *Materials Research Bulletin*, **34**(10/11) (1999) 1637.
5. M. C. HARRIS LIAO, Y. H. CHANG, Y. F. CHEN, J. W. HSU, J. M. LIN and W. C. CHOU, *Appl. Phys. Lett.* **70**(17) (1997) 28.
6. A. RIZZO, M. A. TAGLIENTE, L. CANEVE and S. SCAGLIONE, *Thin Solid Films*, **368** (2000) 8.
7. C. D. LOKHANDE, P. S. PATIL, H. TRIBUTSCH and A. ENNAOUI, *Solar Energy Mater. Solar Cells*, **55** (1998) 379.
8. G. RIVEROS, H. GOMEZ, R. HENRIQUEZ, R. SCHREBLER, R. E. MATROTTI and E. A. DALCHIELE, *Solar Energy Mater. Solar Cells*, **70** (2001) 255.
9. GUOZHEN SHEN, DICHEN, KAIBIN TANG and YITAI QIAN, *J. Cryst. Growth*, **257** (2003) 276.
10. A. M. CHAPARRO, M. A. MARTINEZ, C. GUILLEN, R. BAYON, M. T. GUTIERREZ and J. HERRERO, *Thin Solid Films*, **361/362** (2000) 177.
11. S. VELUMANI, SA. K.NARAYANADASS and D. MANGALARAJ, *Semicond. Sci. Technol.* **13** (1998) 1016.
12. G. B. WILLIAMSON and R. C. SMALLMAN, *Phil. Mag.* **1** (1956) 34.
13. T. MAHALINGAM, J. S. P. CHITRA, J. P. CHU and P. J. SEBASTIAN, *Mater. Lett.* **58** (2004) 1802.
14. P. K. MAHAPATRA, *J. Electrochem. Soc.* **42**(4) (1993) 205.

15. T. S. JEONG, P. Y. YU, K. J. HONG, T. S. KIM, C. J. YOUN, Y. D. CHOI, K. S. LEE, B. O and M. Y. YOON, *J. Cryst. Growth.* **249** (2003) 9.
16. R. KUMARESAN, M. A. ICHIMURA and E. ARAI, *Thin Solid Films.* **414** (2002) 25.
17. C. C. CHANG and C. H. LEE, *ibid.* **379** (2000) 287.
18. HYUN-YONG LEE, SEON-JU KIM, JIN-WOO KIM and HONG-BAY CHUNG, *Thin Solid Films.* **441** (2003) 214.

*Received 28 September 2004  
and accepted 22 July 2005*